# ASSESSING THE PERFORMANCES OF FY-3D/MWRI AND DMSP SSMIS IN GLOBSNOW-2 ASSIMILATION SYSTEM FOR SWE ESTIMATION

*Jianwei Yang[1], Lingmei Jiang[1*], Kari Luojus[2], Juha Lemmetyinen[2], Matias Takala[2]*

1. State Key Laboratory of Remote Sensing Science, Faculty of Geographical Science, Beijing Normal University, Beijing 100875, China
2. Finnish Meteorological Institute, Helsinki Fi00101, Finland

## ABSTRACT

One of the key variables describing global seasonal snow cover is snow water equivalent (SWE). The GlobSnow-2 SWE product is widely used in in many research areas due to the high accuracy level and a long historical record (1979 to the present) in Globally. The satellite data used in GlobSnow-2 are mainly from the Special Sensor Microwave/Imager (SSM/I) and Special Sensor Microwave Imager Sounder (SSMIS). However, there is no launching plan for these sensors in the future. To ensure a continuation of GlobSnow-2 product, this paper assesses the consistency of SWE estimates between the Microwave Radiation Imager (MWRI) and SSMIS in GlobSnow-2 retrieval scheme. The analysis is conducted in three regions (Finland, Russia and China) over the Northern Hemisphere. The results show that the SWE difference between MWRI and SSMIS is small and even can be negligible. This study provides a scientific basis for treating the MWRI dataset as one continuous record.

***Index Terms***— Snow Water Equivalent, GlobSnow-2, FY-3D/MWRI, DMSP/SSMIS, Consistency

## 1. INTRODUCTION

Snow water equivalent (SWE), representing the amount of water stored in the snowpack, is a key variable for hydrological applications, weather prediction, climate change analysis and land surface process simulations [1]. Satellite passive microwave (PMW) data are widely used for the retrieval of SWE because of a wide swath, independent of weather, and a response to the presence of dry snow on land. In addition, there exists a long historical record of spaceborne PMW data dating back to 1978, allowing us to study seasonal snow changes. There are serval entities that use the spaceborne PMW brightness temperature ($T_B$) data to produce SWE products. A technique that assimilates in situ snow depth observations with microwave emissions by means of a forward emission model for snow was proposed by [2]. The European Space Agency (ESA) GlobSnow project has applied this method to produce the Version 2.0 SWE dataset from 1979 to the present for the Northern Hemisphere using the Scanning Multichannel Microwave Radiometer (SMMR), Special Sensor Microwave/Imager (SSM/I) and Special Sensor Microwave Imager/Sounder (SSMIS) data [3]. The GlobSnow-2 SWE product is freely available (www.globsnow.info), and is potentially of great interest to climate change, hydrological processes, permafrost changes, vegetation growth and river runoff [4]. However, there is no launching plan for these sensors (SSM/I and SSMIS) in the near future. The Microwave Radiation Imager (MWRI) onboard the Chinese FengYun-3 (FY-3) series of satellites (FY-3A, 2008; FY-3B, 2010–2019; FY-3C, 2013–the present; FY-3D, 2017–the present) was designed for broad meteorological and environmental applications. Subsequent satellites FY-3E, 3F, and 3G are expected to be launched by 2025. Thus, the MWRI is expected to be one of the candidate sensors.

The primary objectives of this study are to compare the difference of $T_B$ between MWRI and SSMIS over the Northern Hemisphere, to assess the influence of bias in $T_B$ on the SWE estimation for GlobSnow-2 assimilation system and to determine whether the MWRI dataset can be selected as one continuous record to produce long-term SWE data.

## 2. MATERIALS AND METHODS

### 2.1. Satellite passive microwave measurements

The FY-3D satellite was launched on 15 November 2017 and it is in a sun-synchronous orbit with local ascending overpasses at about 2:00 p.m. The MWRI sensor loaded in the FY-3D is a 10-channel, 5-frequency, 2-polarization radiometer system that measures $T_B$ ranging from 10.65 to 89 GHz at horizontal and vertical polarizations (http://satellite.nsmc.org.cn). The SSMIS has provided continuous measurements at 19.35, 23.235, 37 and 91.655 GHz since November 2006 (https://daacdata.apps.nsidc.org). Both the vertical and horizontal polarizations are measured, except at 23.235 GHz, where only the vertical polarization is measured. In this study, only the satellite observations at approximately 19 GHz and 37 GHz in vertical polarization

were assimilated into the GlobSnow-2. To enhances the spatial coverage, data used in GlobSnow-2 is a combination of ascending and descending orbital nodes.

### 2.2. Reference datasets for evaluation

Three independent reference datasets from China, Russia and Finland were used to assess the consistency in SWE for GlobSnow-2 assimilation system in this study.

*(1) China's reference dataset*

The weather station daily data in China from January to May 2018 were provided by the National Meteorological Information Centre, China Meteorology Administration (Fig. 1). The recorded variables include the site name, geolocation (latitude and longitude) and snow depth (cm). Here, snow density is treated with a constant value of 240 kg/m$^3$ to transfer snow depth to SWE. We collected appropriately 7,000 records in China as evaluation data.

*(2) Snow surveys data from Russia*

The dataset has routine snow surveys that run throughout the cold season every 10 days (every five days during the intense snowmelt) at 517 meteorological stations (Fig. 1) of Russia (http://meteo.ru/english/data/). Snow surveys ran separately along all types of environment typical for the site for 1 to 2 km. At each 10 to 20 meters the snow depth was measured and at each 100 to 200 meters a snow density sampling was conducted. SWE was calculated as a product of snow depth and averaged snow density. A total of 6,000 samples were collected as evaluation data.

*(3) Snow course data from Finland*

Finland has a comprehensive network of 139 snow survey sites (Fig. 1) operated by the Finnish Environment Institute (SYKE). The SWE measurement was made once or twice in every month. Each snow course is 2 to 4 km long, covering the various land cover types. The measurement procedure is similar to that of snow surveys in Russia. Appropriately 500 samples were collected to assess the SWE estimates.

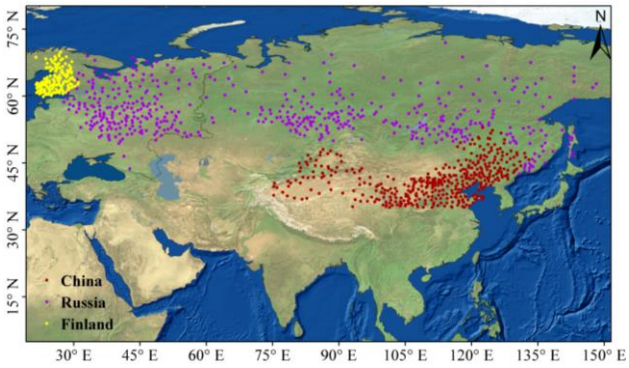


Fig.1 Spatial distribution of the weather stations in three regions over the Northern Hemisphere (> 35º N).

### 2.3. Methodology

The methodology for SWE retrieve was overviewed in [3]. This approach takes into account atmospheric and forest effects to space-borne measurement by means of the forest transmissivity model by [5] and statistical atmospheric model in [6]. The optimization of effective snow grain size is conducted by fitting forward model (HUT) predictions to the satellite observations at approximately 19 and 37 GHz. A map of spatially continuous 'assimilated SWE' is produced though a Bayesian non-linear iterative assimilation approach first described in [2].

Fig. 2 shows the assessment process in this study. Satellite observations from the MWRI and SSMIS sensors during the period January-May 2018 were used to retrieve SWE though the assimilation algorithm. We compared the differences in $T_B$ between MWRI and SSMIS over the Northern Hemisphere. Three independent reference SWE datasets were applied to assess the consistency of assimilated SWE products with MWRI and SSMIS (hereafter, GS@MWRI and GS@SSMIS, respectively).

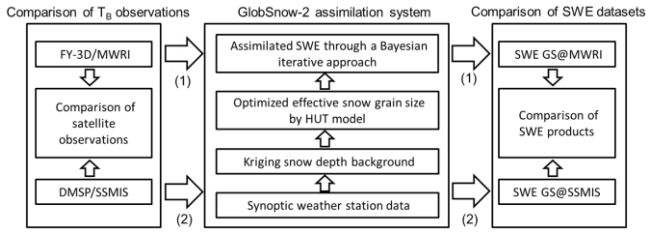


Fig.2 Flowchart of the assessment procedure in this study.

## 3. RESULTS

### 3.1. Comparison of $T_B$ between MWRI and SSMIS

Table 1 shows the overall mean bias of $T_B$ between MWRI and SSMIS under snow possible areas. The $T_B$ from MWRI at 19 GHz tends to be larger than the observation of SSMIS, with mean biases of 3.6 K and 2.0 K for the ascending and descending, respectively. For the 37 GHz, the mean biases are minus, with mean biases of -0.3 K and -3.1 K for the ascending and descending orbits, respectively.

Table 1. Summary of overall mean bias (MWRI - SSMIS).

| Mean Bias (K) | | | |
|---|---|---|---|
| Frequency | Polarization | Ascending | Descending |
| 19 GHz | V | 3.6 | 2.0 |
| 37 GHz | V | -0.3 | -3.1 |

The spatial patterns of bias in $T_B$ are shown in Fig. 3. MWRI tends to yield a higher $T_B$ than SSMIS for the 19 GHz channel (Fig. 3a). The biases in middle-low latitudes (< 54º N) are larger than these in high latitudes (> 54º N) for the 19VA (vertical polarization and ascending orbit) channel. For the 37 GHz channel, the patterns of bias in middle-low and high latitude areas are converse, especially for the ascending node (Fig. 3b). The biases are minus in high latitude areas, whereas they are positive in middle-low latitude areas for the ascending node. The pattern of bias

depends on the latitude for the ascending node (e.g., 19VA and 37VA channels).

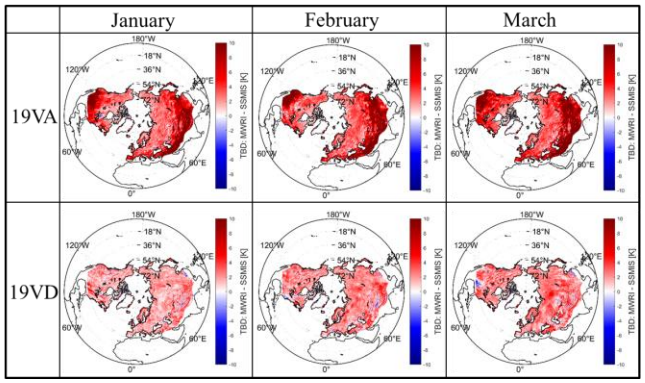


(a)

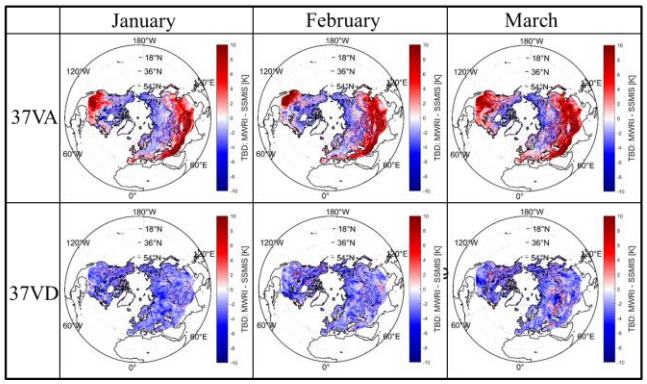


(b)

Fig.3 Spatial distribution of the bias between MWRI and SSMIS at (a) 19 GHz, and (b) 37 GHz in vertical polarization (V) for ascending (A) and descending (D) nodes.

### 3.2. Assessment of consistency in SWE estimation

*3.2.1. Finland*

Fig. 4 shows the scatter plots of GS@MWRI and GS@SSMIS products compared with the reference dataset in Finland. Both products present similar performances with respect to correlation coefficient, RMSE, unbiased RMSE and mean bias. The results indicate that the consistency of both products is well in Finland.

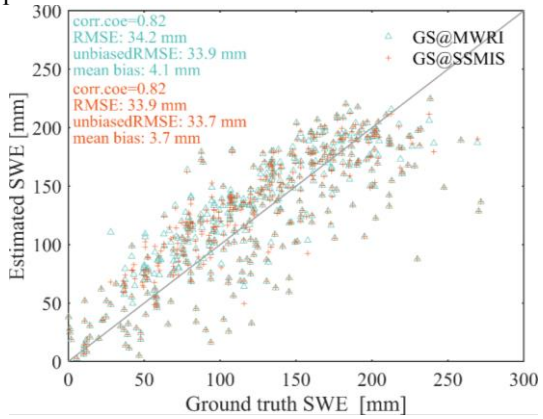


Fig.4 The comparison of two SWE products (GS@MWRI *vs.* GS@SSMIS) retrieved with GlobSnow-2 algorithm.

Fig. 5 shows the time series of daily mean SWE estimates and station observations. Both colorful solid lines display that the temporal patterns of two products are similar. Black solid line presents the variation of weather station observations. Both products tend to overestimate SWE during the period January-March and underestimate SWE at the end of April.

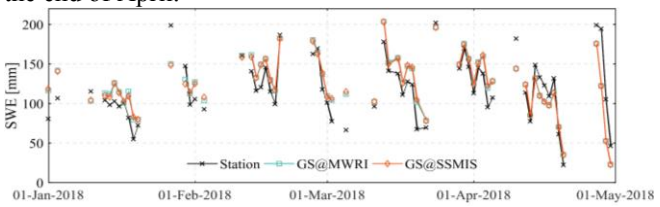


Fig.5 Time series of daily mean estimated SWE and ground truth value in Finland.

*3.2.2. Russia*

Fig. 6 shows the performances of two SWE products in Russia. Both products present notable underestimation under deep snow conditions (when SWE exceeds ~ 200 mm). However, the consistency of two products is well, with a high correlation coefficient of 0.99.

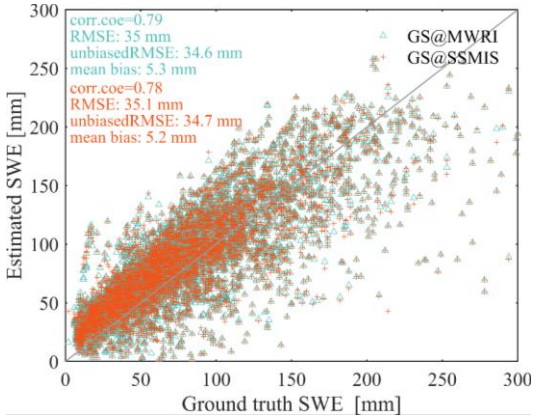


Fig.6 The comparison of two SWE products (GS@MWRI *vs.* GS@SSMIS) retrieved with GlobSnow-2 algorithm.

Time series of daily mean SWE estimates and station observations in Russia are shown in Fig. 7. Both products present similar patterns and they tend to overestimate SWE from January to March compared with the ground truth observation. The daily mean SWE is largest in April among snow season months. GlobSnow-2 algorithm presents a notable underestimation in April.

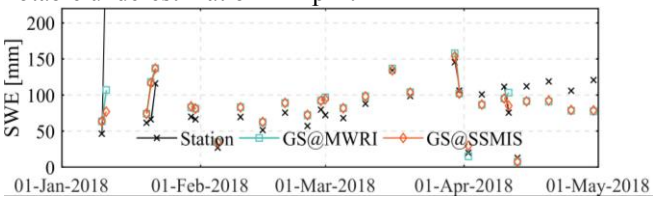


Fig.7 Time series of estimated and observed SWE in Russia.

*3.2.3. China*

Fig. 8 shows the time series of correlation coefficient, mean bias, and unbiased RMSE compared with station data in China. The temporally patterns are similar for two products, suggesting a well consistency of them. The correlation coefficient presents a decreasing trend from January to May (Fig. 8a). The mean bias and unbiased RMSE are lower in the beginning of snow season than later in the winter (Fig. 8b and 8c). The mean bias increases from approximately 0 mm to 30 mm and the unbiased RMSE from approximately 15 mm to 33 mm in China, suggesting that the GlobSnow-2 algorithm has problems for the SWE estimation in the late of snow season in China.

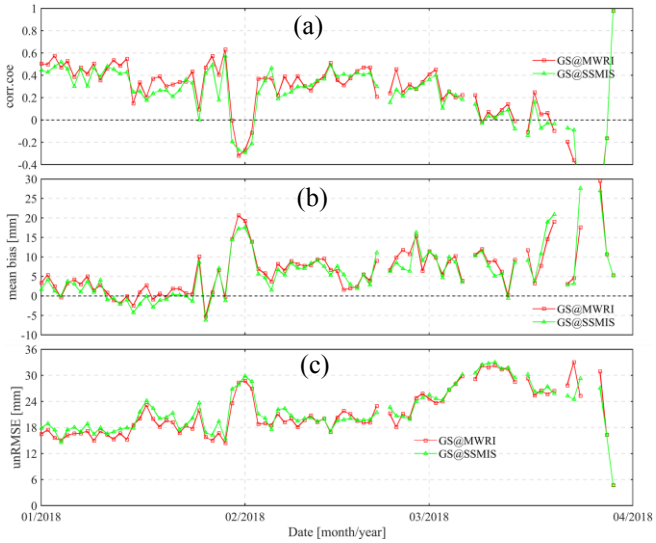


Fig. 8 Time-series of (a) correlation, (b) mean bias, and (c) unbiased RMSE compared with station data in China.

## 4. DISCUSSION

The results in Section 3 present a decrease in the SWE accuracy, especially at the end of snow season. Fig. 5 and Fig. 7 indicate that there is notable underestimation at the end of snow season in Finland and Russia. This is because the snow cover is thick and the stratigraphic parameters become large (e.g. snow density), which leads to the limited penetration depth at 37 GHz, namely, saturation effect. Fig. 8 indicates that GlobSnow-2 product tend to overestimate SWE since February in China. The snow cover in China is generally shallow, with a mean SWE of approximately 25 mm. The saturation effect should not occur for most snow conditions. Thus, the snow metamorphism is the dominant factor that leads to the strong scatter effects and a large $T_B$ gradient. The GlobSnow-2 SWE retrieval scheme utilized a fixed density of 240 kg/m$^3$. While based on ground truth data, the average snow density in China is 180 kg/m$^3$ [7]. There is no doubt that using a fixed snow density to convert from snow depth to SWE results in overestimation in China.

There are notable $T_B$ differences between the MWRI and SSMIS (Table 1 and Fig. 3). However, the influence of these biases on SWE estimation for GlobSnow-2 assimilation system is small and even can be negligible in Globally. The snow grain size is a very important parameter within the forward $T_B$ simulation component of the retrieve. The effective grain size optimized by fitting the modeled $T_B$ into satellite observation is actually an effective value that includes the effect of modeling errors and uncertainties in input data [3]. Thus, the inconsistency in SWE estimation caused by the biases of two sensors' observations is poor.

## 5. CONCLUSION

In this study, we compared the difference of $T_B$ between MWRI and SSMIS and analyzed the SWE consistency of GS@MWRI and GS@SSMIS products retrieved with GlobSnow-2 algorithm but different satellite data. We concluded that the spatial pattern of $T_B$ bias depends on the latitude for the ascending orbital node and that the SWE difference caused by the $T_B$ bias of MWRI and SSMIS is small and even can be negligible due to the implementation of optimizing effective snow grain size in GlobSnow-2. This study provides a scientific basis for treating the MWRI dataset as one of the candidate continuous satellite records.

## 6. ACKNOWLEDGEMENTS

This study is jointly supported by the National Natural Science Foundation of China (41671334), the National Basic Survey Program of China (2017FY100502).

## 7. REFERENCES

[1] C. Derksen, P. Toose, A. Rees, L. Wang, M. English, A. Walker, and M. Sturm, "Development of a tundra-specific snow water equivalent retrieval algorithm for satellite passive microwave data," R Remote Sens. Environ, 114. 1699–1709, 2010.

[2] J. Pulliainen, "Mapping of snow water equivalent and snow depth in boreal and sub-arctic zones by assimilating space-borne microwave radiometer data and ground-based observations," Remote Sens. Environ, 101. 257–269, 2006.

[3] M. Takala, K. Luojus, J. Pulliainen, J. Lemmetyinen, K. Juha-Petri, J. Koskinen, B. Bojkov, "Estimating northern hemisphere snow water equivalent for climate research through assimilation of space-borne radiometer data and ground-based measurements," Remote Sens. Environ, 115. 3517–3529, 2011.

[4] F. Larue, A. Royer, D. DeSève, A. Langlois, A. Roy, L. Brucker, "Validation of GlobSnow-2 snow water equivalent over Eastern Canada," Remote Sens. Environ, 194. 264–277, 2017.

[5] N. Kruopis, J. Praks, A. Arslan, H. Alasalmi, J. Koskinen, and M. Hallikainen, "Passive microwave measurements of snow-covered forests in EMAC'95," IEEE Trans. Geosci. Remote Sens, 37. 2699−2705, 1999.

[6] J. Pulliainen, J.P. Kärnä, and M.T. Hallikainen, "Development of geophysical retrieval algorithms for the MIMR," IEEE Trans. Geosci. Remote Sensing, 31. 268–277, 1993.

[7] J.W. Yang, L.M. Jiang, S.L. Wu, G.X. Wang, J. Wang, and X.J. Liu, "Development of a Snow Depth Estimation Algorithm over China for the FY-3D/MWRI," Remote Sensing, 11. 977, 2019.